# REPORT DOCUMENTATION PAGE

| 1. REPORT DATE *(DD-MM-YYYY)* | 2. REPORT TYPE Technical Papers | 3. DATES COVERED *(From - To)* |
|---|---|---|

**4. TITLE AND SUBTITLE**

**5a. CONTRACT NUMBER**

**5b. GRANT NUMBER**

**5c. PROGRAM ELEMENT NUMBER**

**6. AUTHOR(S)**

**5d. PROJECT NUMBER**
2303

**5e. TASK NUMBER**
M2C8

**5f. WORK UNIT NUMBER**

**7. PERFORMING ORGANIZATION NAME(S) AND ADDRESS(ES)**

Air Force Research Laboratory (AFMC)
AFRL/PRS
5 Pollux Drive
Edwards AFB CA 93524-7048

**8. PERFORMING ORGANIZATION REPORT**

**9. SPONSORING / MONITORING AGENCY NAME(S) AND ADDRESS(ES)**

Air Force Research Laboratory (AFMC)
AFRL/PRS
5 Pollux Drive
Edwards AFB CA 93524-7048

**10. SPONSOR/MONITOR'S ACRONYM(S)**

**11. SPONSOR/MONITOR'S NUMBER(S)**

**12. DISTRIBUTION / AVAILABILITY STATEMENT**

Approved for public release; distribution unlimited.

**13. SUPPLEMENTARY NOTES**

**14. ABSTRACT**

**15. SUBJECT TERMS**

**16. SECURITY CLASSIFICATION OF:**

| a. REPORT | b. ABSTRACT | c. THIS PAGE | 17. LIMITATION OF ABSTRACT | 18. NUMBER OF PAGES | 19a. NAME OF RESPONSIBLE PERSON Leilani Richardson |
|---|---|---|---|---|---|
| Unclassified | Unclassified | Unclassified | A | | 19b. TELEPHONE NUMBER *(include area code)* (661) 275-5015 |

Standard Form 298 (Rev. 8-98)
Prescribed by ANSI Std. 239.18

TP-FY99-Ø113

✓ Sponsored
✓ DTS

MEMORANDUM FOR PRS

FROM: PROI (TI) (STINFO)

28 May 1999

SUBJECT: Authorization for Release of Technical Information, Control Number: **AFRL-PR-ED-TP-FY99-0113**
C.W. Larson, "Kinetics of Boron Carbon HEDM"

Presented to HEDM Conference

(Statement A)

*of formation/reaction*

# Kinetics of Boron Carbon HEDM

C. W. Larson,
Air Force Research Laboratory,
Edwards AFB, CA 93524-7680

HEDM Contractors' Conference
Cocoa Beach, FL
7 June - 11 June 1999
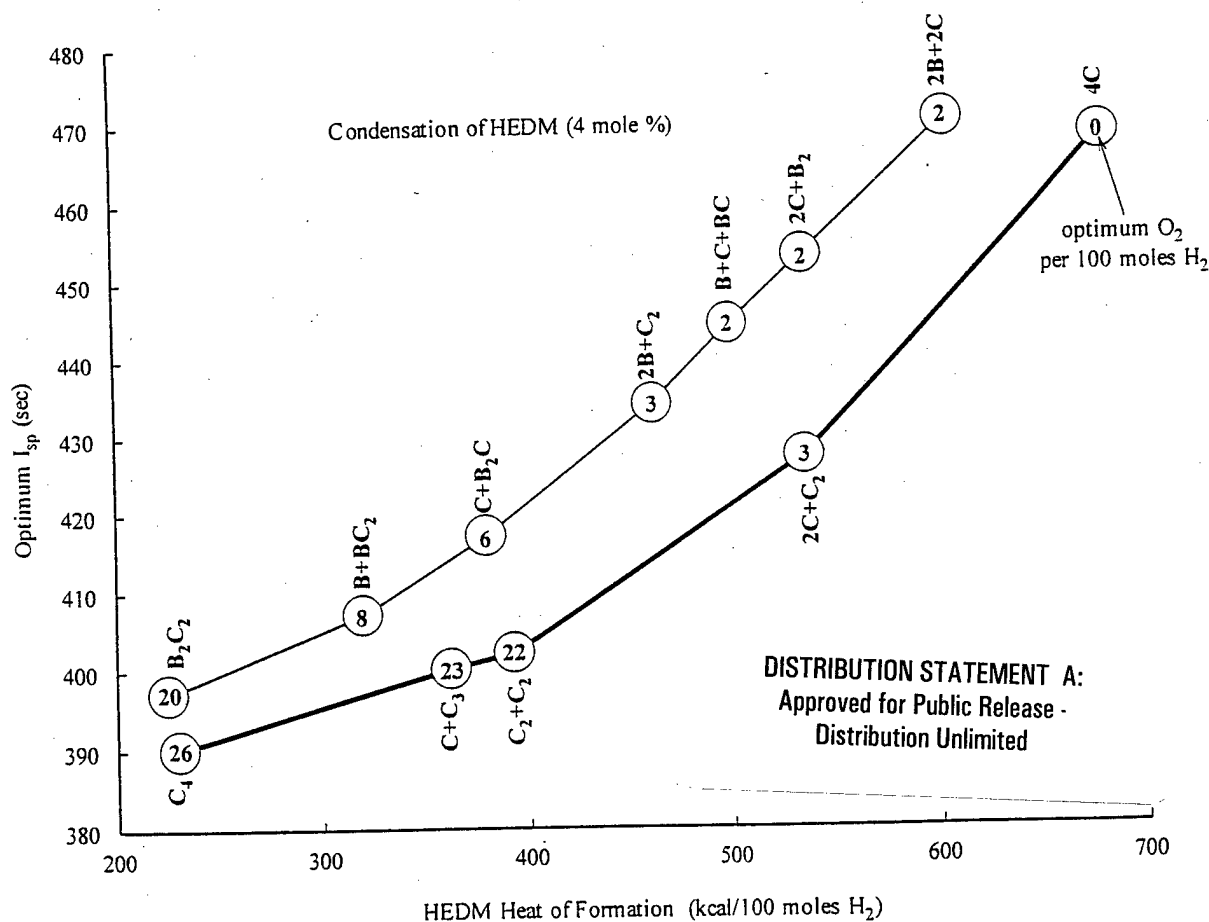


Figure 1. Specific impulse of HEDM containing 4 mole percent equivalent atom density in solid hydrogen with various stages of condensation. Numbers inside circles denote the optimum moles of $O_2$ per 100 moles of $H_2$ that produces the maximum Isp for the indicated compositions. The calculations are based on the standard rocket operating conditions, 1000 psi combustion pressure and 1 atm nozzle exit pressure, which produce 389 sec with liquid oxygen/liquid hydrogen propellant. The propellant composed of 4 mole percent C-atoms produces maximum Isp with no oxygen. If the atoms condense to 1 mole percent C4, the Isp drops to the baseline 389 sec value.

# Objective - 5% atoms in cryogenic matrix

## Approach

1. FTIR spectroscopy of $B_JC_{n-J}$ clusters isolated in 10 K argon matrix

2. Ab-initio calculations of cluster
   (a) normal mode frequencies and frequency shifts of their isotopomers
   (b) infrared absorption intensities (km mol$^{-1}$)

3. Measurement of cluster distributions produced upon deposition and after annealing. Absolute column densities (molecules cm$^{-2}$) from Beer's Law

$$< \rho_i l > = \frac{A_{exp}}{I_{theory}} N$$

$$A_{exp} = -\int_{\nu} \ln\left[\frac{E_t(\nu)}{E_0(\nu)}\right] d\nu$$

$B_JC_{n-J}$
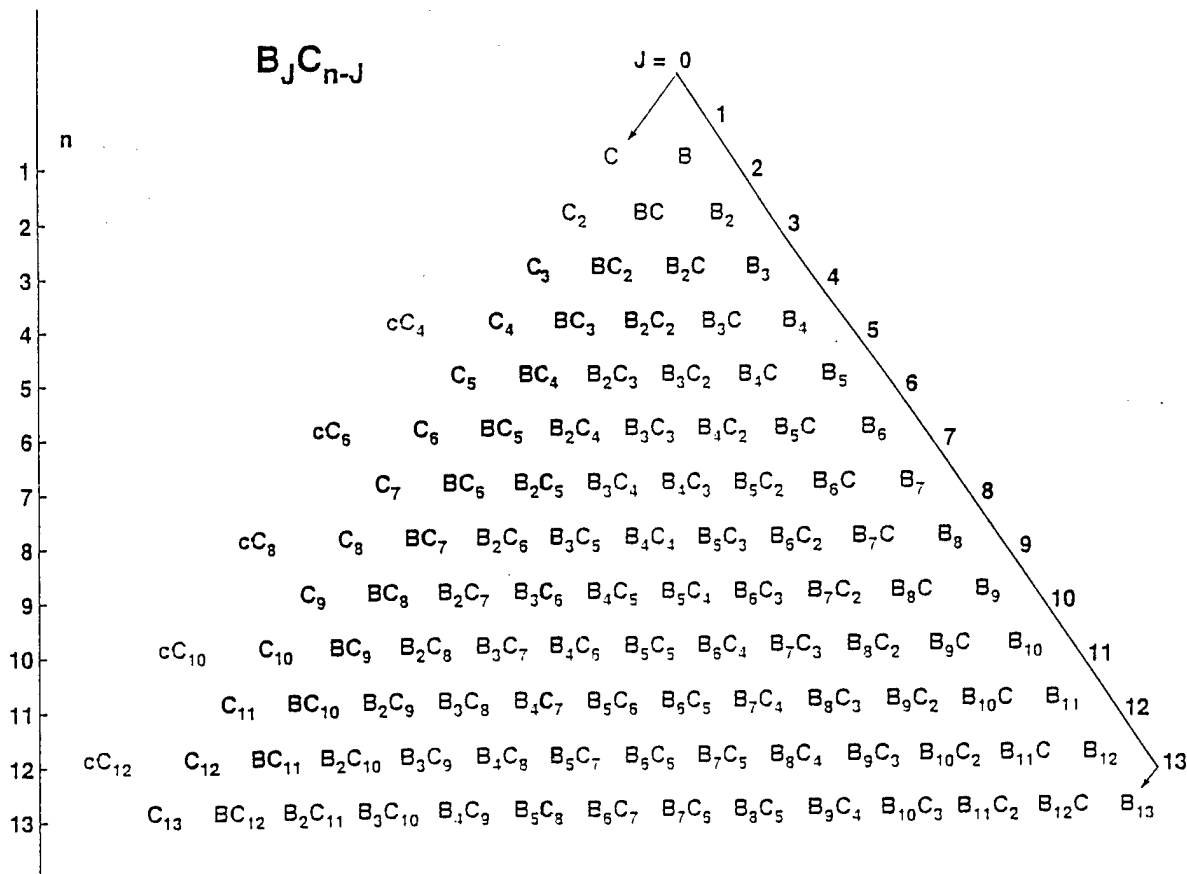
FIG. 1. FTIR spectra of the $\nu_2(\sigma)$ mode of isotopomers of linear $BC_3$ and the $\nu_3(\sigma_u)$ mode of isotopomers of linear $C_4$. The spectra were recorded at 10 K after annealing the matrices with the indicate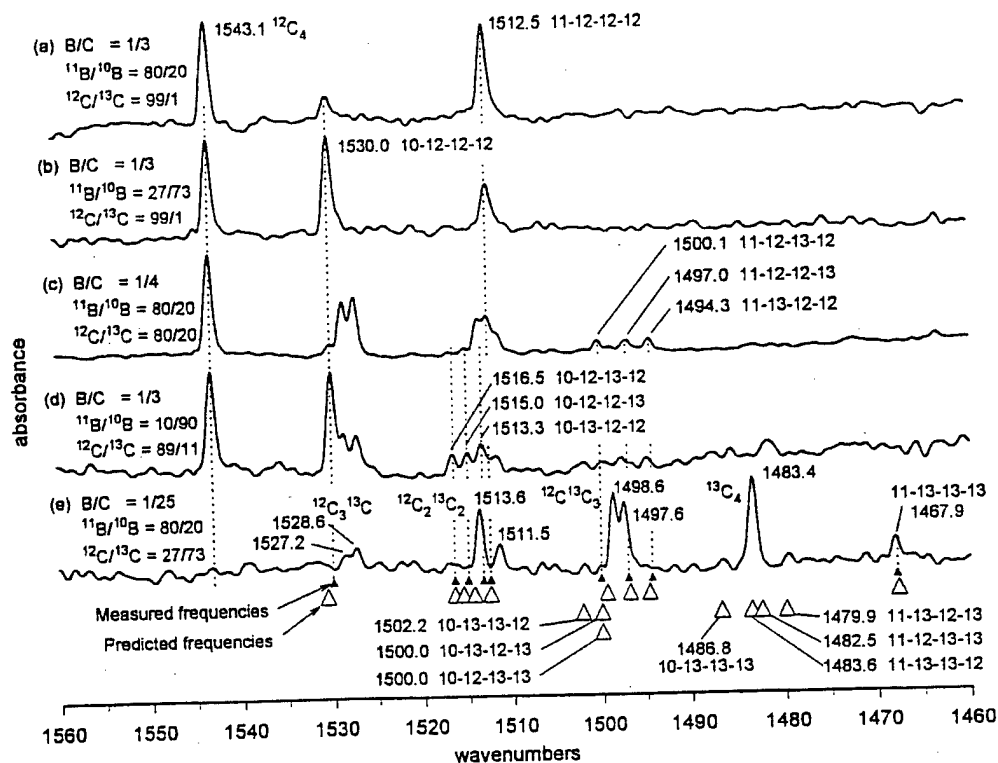d compositions at 27.5 K for 150 s. The large open triangles at the bottom show the predicted frequencies of linear $BC_3$ isotopomers (as explained in the text) and small filled triangles show measured isotopomer frequencies.
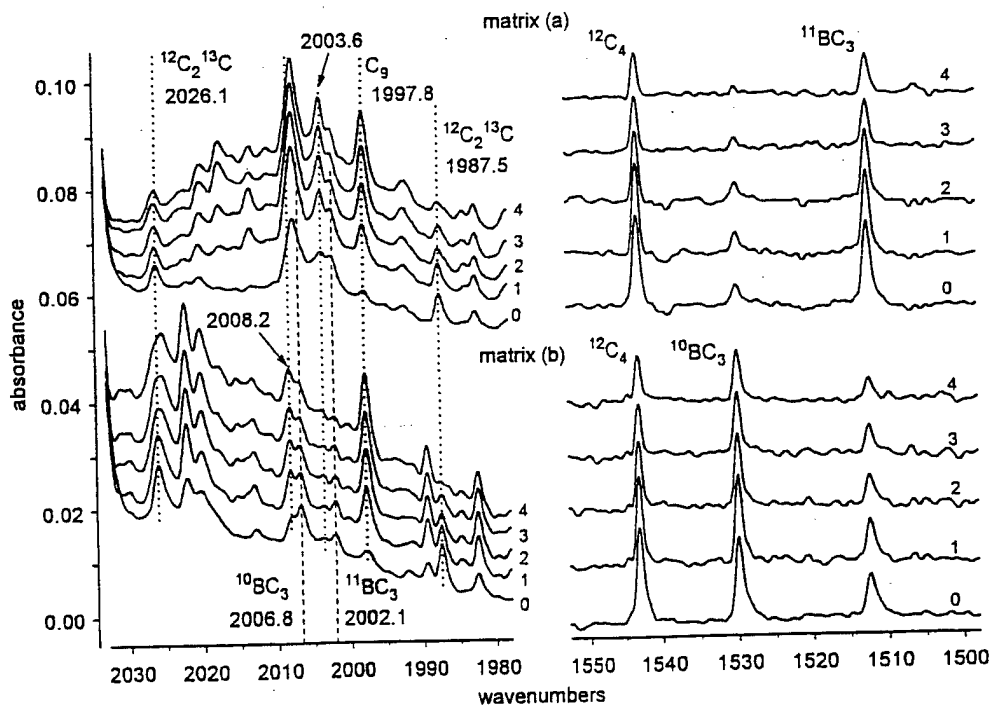


FIG. 2. Spectra obtained from matrix (a) [$^{11}B/^{10}B = 4/1$] and matrix (b) [$^{11}B/^{10}B = 1/2.7$] showing correlation upon annealing of the $\nu_1(\sigma)$ bands of $^{10}BC_3$ and $^{11}BC_3$ at 2006.8 and 2002.1 $cm^{-1}$ with the $\nu_2(\sigma)$ bands at 1530.0 and 1512.5 $cm^{-1}$. The spectra labeled "0" are from the originally deposited matrix. Labels "1" to "4" indicate spectra recorded after the first through fourth annealing as follows: (1) 27.5 K for 150 s. (2) 30.0 K for 75 s. (3) 32.5 K for 45 s. (4) 35.0 K for 30 s. Frequency and absorbance scales are identical for all spectra. The plotted absorbance is $-\log_{10}$ of the transmittance. To facilitate comparisons between matrices, the absorbance of the matrix (b) spectra are multiplied by 1.4.

3

(a) B/C = 1/3
$^{11}B/^{10}B = 80/20$
$^{12}C/^{13}C = 99/1$

955.0 11-12-12-11

967.7 11-12-12-10

(b) B/C = 1/3
$^{11}B/^{10}B = 27/73$
$^{12}C/^{13}C = 99/1$

979.0 10-12-12-10

(c) B/C = 1/4
$^{11}B/^{10}B = 80/20$
$^{12}C/^{13}C = 80/20$

945.8 11-12-13-11

absorbance

(d) B/C = 1/3
$^{11}B/^{10}B = 10/90$
$^{12}C/^{13}C = 89/11$

970.2 10-12-13-10

(e) B/C = 1/25
$^{11}B/^{10}B = 80/20$
$^{12}C/^{13}C = 27/73$

950.6 11-13-13-10

937.5 11-13-13-11

Measured frequencies
Predicted frequencies

958.5 11-13-12-10
959.1 11-12-13-10
962.1 10-13-13-10

990   980   970   960   950   940   930
wavenumbers

FIG. 3. FTIR spectra of the $\nu_3(\sigma_u)$ mode of isotopomers of linear BCCB. The spectra were recorded after annealing the matrices with the indicated compositions at 27.5 K for 150 s. The large open triangles at the bottom show the predicted frequencies of linear BCCB isotopomers (as explained in the text) and small filled triangles show measured isotopomer frequencies.
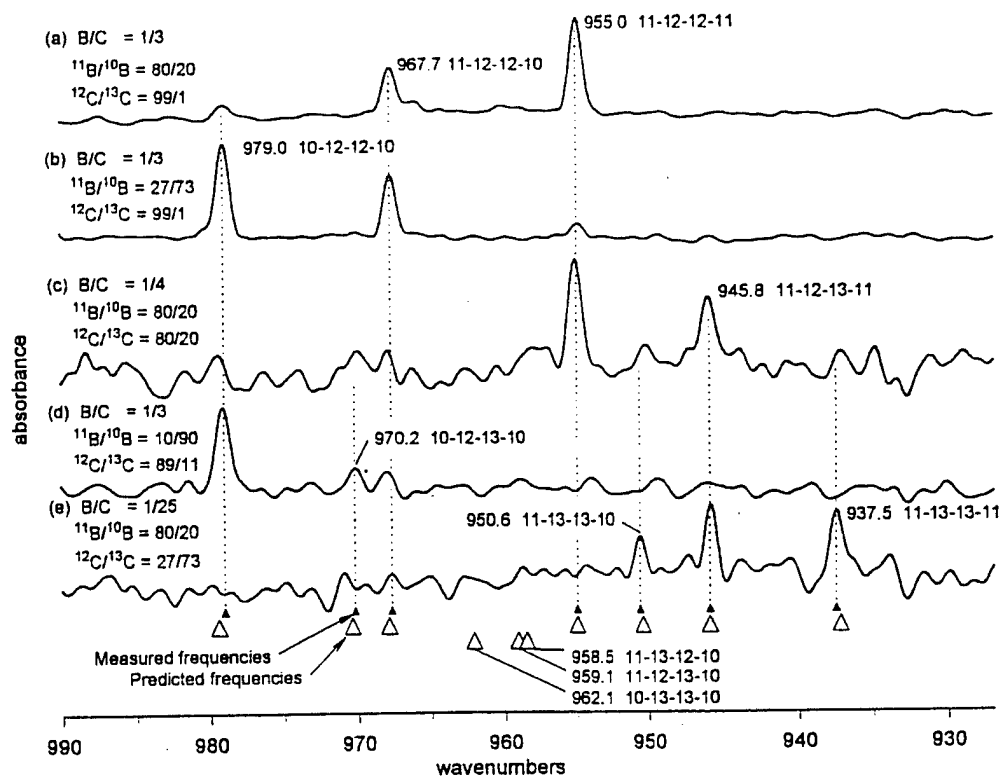
TABLE IV. Experimental $B_2C_2$ isotopomer frequency patterns. Frequencies and frequency intervals (cm$^{-1}$) in triplet bands of $B_2C_2$ isotopomers.

| Boron isotope triplets | | | | Carbon isotope triplets | | | |
| --- | --- | --- | --- | --- | --- | --- | --- |
| | | Intervals | | | | Intervals | |
| Isotopomer | Freq. | Short | Long | Isotopomer | Freq. | Short | Long |
| $^{10}B_2\,^{12}C_2$ | 979.0 | | | $^{10}B_2\,^{12}C_2$ | 979.0 | | |
| | | 11.3 | | | | 8.8 | |
| $^{10,11}B_2\,^{12}C_2$ | 967.7 | | 24.0 | $^{10}B_2\,^{12,13}C_2$ | 970.2 | | (16.7)[a] |
| | | 12.7 | | | | (7.9)[a] | |
| $^{11}B_2\,^{12}C_2$ | 955.0 | | | $^{10}B_2\,^{13}C_2$ | (962.3)[a] | | |
| $^{10}B_2\,^{12,13}C_2$ | 970.2 | | | $^{10,11}B_2\,^{12}C_2$ | 967.7 | | |
| | | (11.5)[a] | | | | (9.0)[a] | |
| $^{10,11}B_2\,^{12,13}C_2$ | (958.7)[a] | | 24.4 | $^{10,11}B_2\,^{12,13}C_2$ | (958.7)[a] | | 17.1 |
| | | (12.9)[a] | | | | (8.1)[a] | |
| $^{11}B_2\,^{12,13}C_2$ | 945.8 | | | $^{10,11}B_2\,^{13}C_2$ | 950.6 | | |
| $^{10}B_2\,^{13}C_2$ | (962.3)[a] | | | $^{11}B_2\,^{12}C_2$ | 955.0 | | |
| | | (11.7)[a] | | | | 9.2 | |
| $^{10,11}B_2\,^{13}C_2$ | 950.6 | | (24.8)[a] | $^{11}B_2\,^{12,13}C_2$ | 945.8 | | 17.5 |
| | | 13.1 | | | | 8.3 | |
| $^{11}B_2\,^{13}C_2$ | 937.5 | | | $^{11}B_2\,^{13}C_2$ | 937.5 | | |

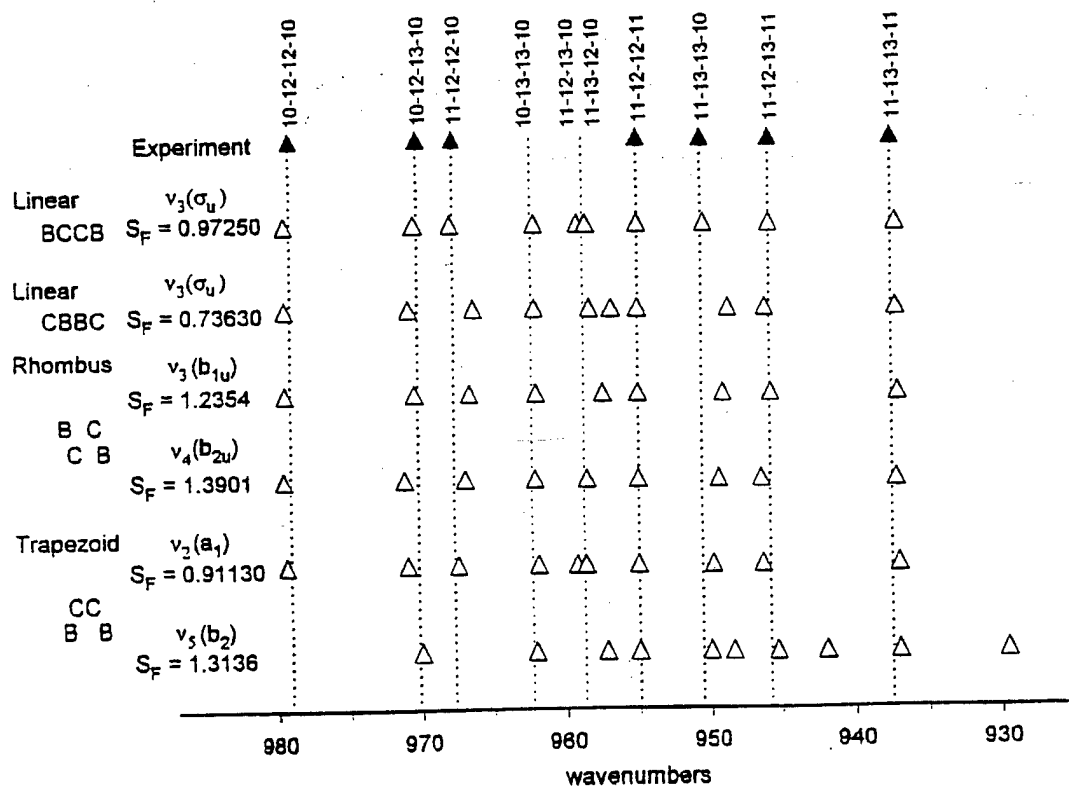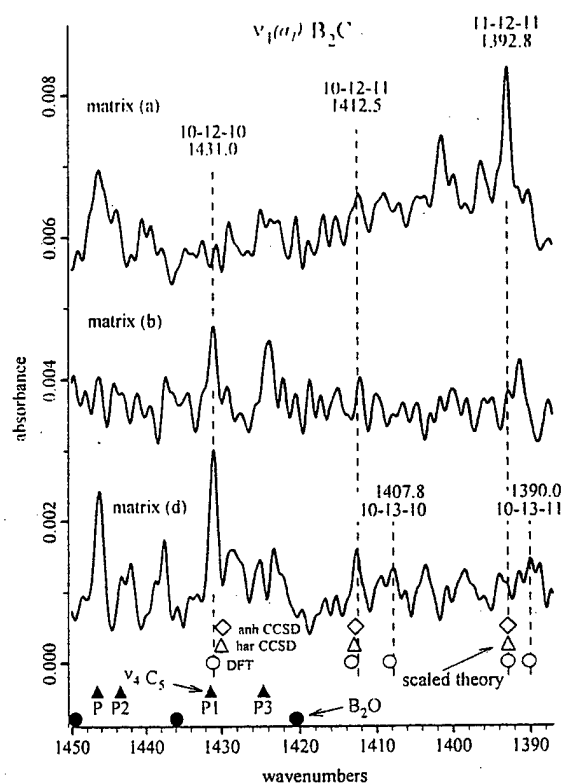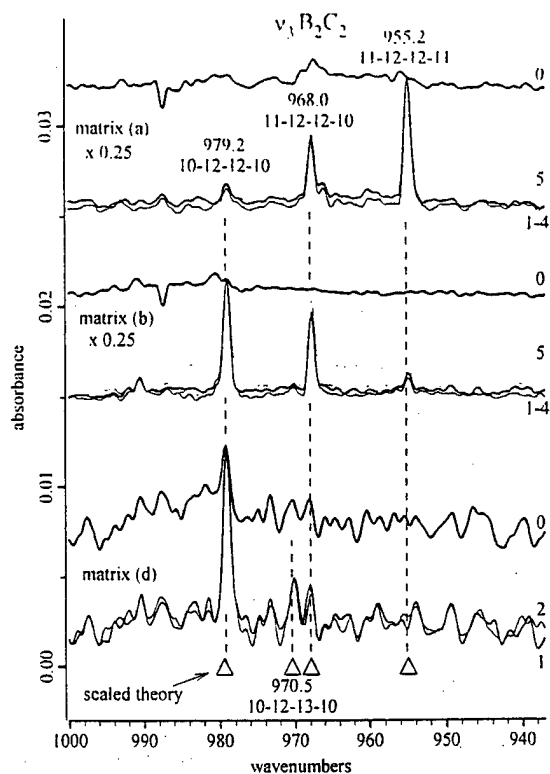[a]Frequencies and intervals in parentheses were interpolated or extrapolated from measured quantities.
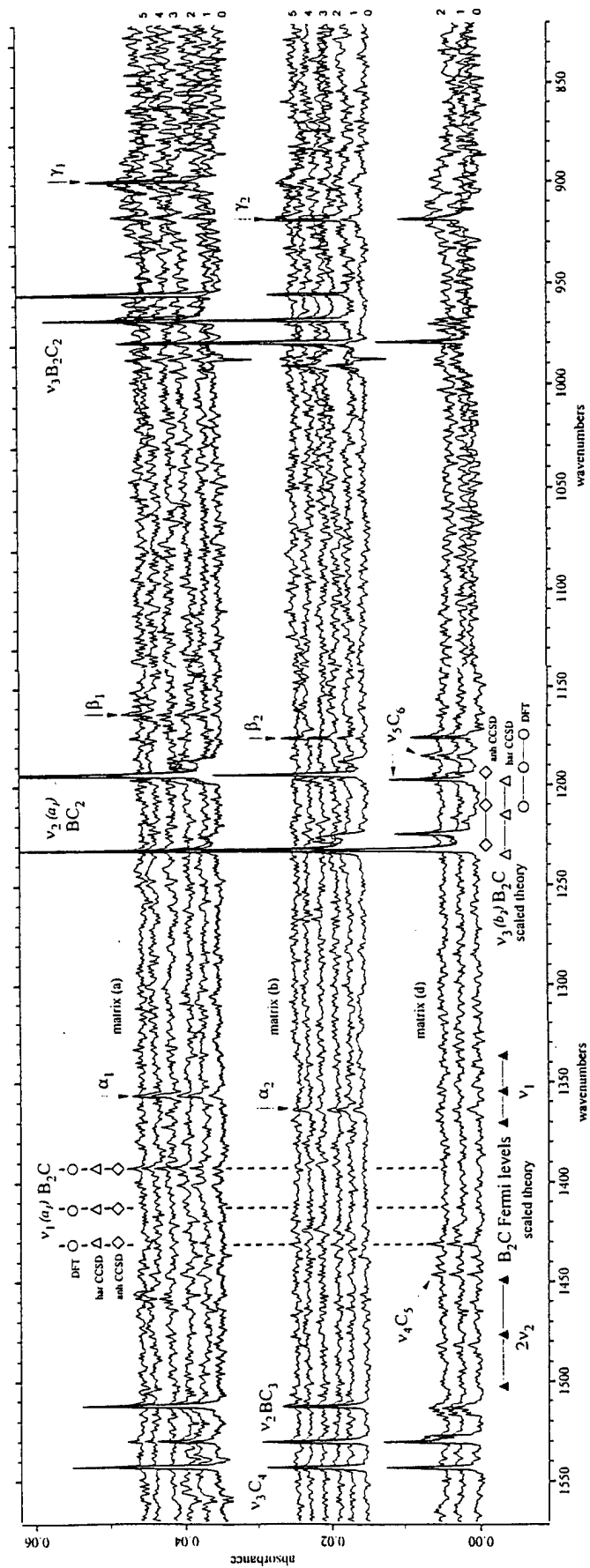
FIG. 4. Comparison of experimental isotopomer frequencies to scaled theoretical isotopomer frequencies for the most intense modes of four $B_2C_2$ geometries as calculated by Rittby. Ref. 5.
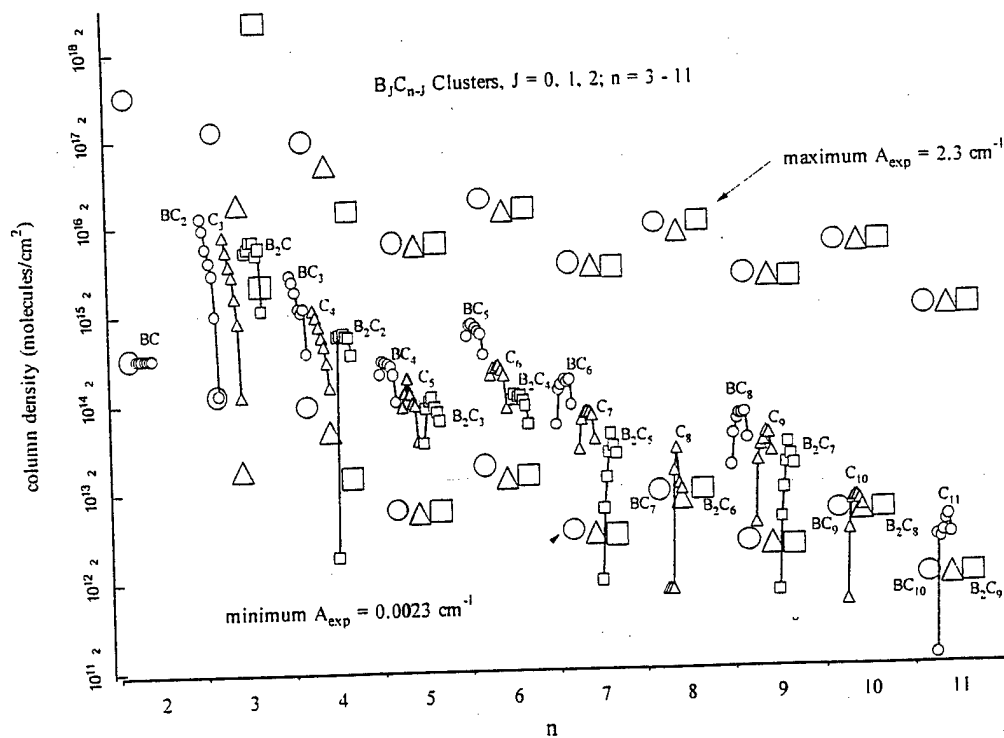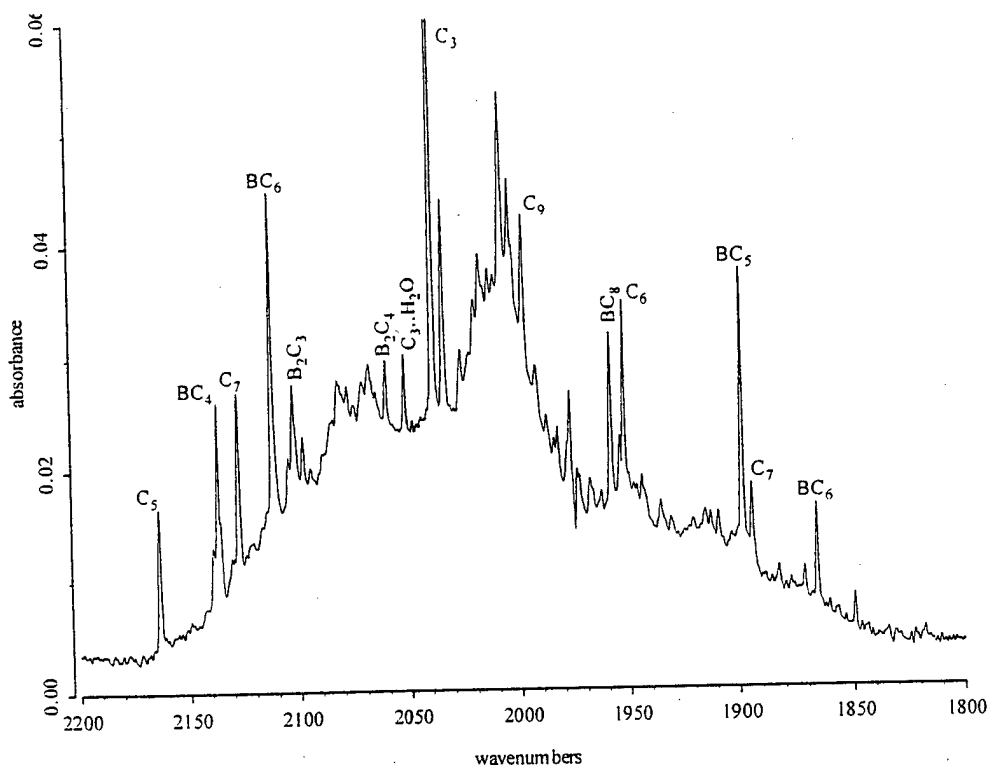
Figure 1. Distribution of $B_jC_{n-j}$ clusters. $J = 0, 1, 2; n = 3 - 11$. Circles, triangles and squares represent $BC_{n-1}$, $C_n$, and $BC_{n-2}$ clusters, respectively. Large symbols denote upper and lower limits of measurement, based on a nominal minimum measurable absorbance of 0.0023 $cm^{-1}$, and a maximum absorbance for linearity of Beer's law of 2.3 $cm^{-1}$ (1% transmittance. Small symbols denote measured quantities in the initial matrix, and in six annealed matrices. Annealing temperatures and times were (1) 27.5 K/150 s, (2) 30.0 K/75 s, (3) 32.5 K/45 s, (4) 35.0 K/30 s, (5) 37.5 K/20 s, (6) 40.0 K/20 s. The decreases in column density in the fifth and sixth annealing are due to matrix sublimation. Some of the larger clusters (n = 8, 10, 11) have not been identified. $BC_7$, $B_2C_6$, $BC_9$, $B_2C_8$, $BC_{10}$, $B_2C_9$.

$C_3$ — 6, 5, 4, 3, 2, 1, 0 — 0.2, 0.0 — 2040 2035 2030

$^{11}BC_2$ — 0.06, 0.00 — 1197 1192 1187

$^{11}B_2C$ — 0.002, 0.000 — 1398 1393 1388

annealing — 0 1 2 3 4 5 6

$C_4$ — 6, 5, 4, 3, 2, 1, 0 — 0.015, 0.000 — 1548 1543 1538

$^{11}BC_3$ — 0.015, 0.00 — 1517 1512 1507

$^{11}B_2C_2$ — 0.03 — 960 955 950

$C_5$ — 6, 0, 5, 4, 3, 1, 2 — 0.015, 0.000 — 2169 2164 2159

$^{11}BC_4$ — 6, 0, 5, 4, 1, 2, 3 — 0.02, 0.00 — 2141 2136 2131

$^{11}B_2C_3$ — 0, 6, 5, 1, 1, 4, 3, 2 — 0.013, 0.000 — 2108 2103 2098

annealing — 0 1 2 3 4 5 6

$C_6$ — 6, 0, 5, 3, 4, 1, 2 — 0.02, 0.00 — 1957 1952 1947

$^{11}BC_5$ — 6, 0, 5, 1, 2, 4, 3 — 0.03, 0.00 — 1903 1898 1893

$^{11}B_2C_4$ — 6, 0, 1, 2, 3, 4 — 0.006, 0.000 — 2065 2060 2055

annealing — 0 1 2 3 4 5 6

$C_7$ — 0, 6, 1, 2, 5, 4, 3 — 0.02, 0.00 — 2132 2127 2122

$^{11}BC_6$ — 0, 6, 1, 2, 4, 3, 5 — 0.035, 0.000 — 2117 2112 2107

$^{11}B_2C_5$ — 0, 6, 1, 5, 4, 3, 2 — 0.004, 0.000 — 1854 1849 1844

$C_9$ — 0, 6, 1, 2, 3, 5, 4 — 0.02, 0.00 — 2003 1998 1993

$^{11}BC_8$ — 0, 6, 1, 2, 3, 5, 4 — 0.015, 0.000 — 1963 1958 1953

$^{11}B_2C_7$ — 0, 1, 6, 2, 3, 4, 5 — 0.005, 0.000 — 2103 2098 2093

matrix (a) 0 1 C$_5$
5 4 3 2
6

matrix (b) 0 1
5 4 3 2

0.04
0.02
0.00

BC$_4$
C$_7$
BC$_6$
B$_2$C$_3$

2160
2140
wavenmbers
2120
2100

BC6rg3D May 28, 1999 8:32:14 AM



0.04
0.02
0.00

matrix (a) 0
5 4 3 2 1
6

matrix (b) 0
5 4 3 2 1

$^{10}$B$_2$C$_2$
$^{10,11}$B$_2$C$_2$
$^{11}$B$_2$C$_2$

990
980
970
wavenmbers
960
950
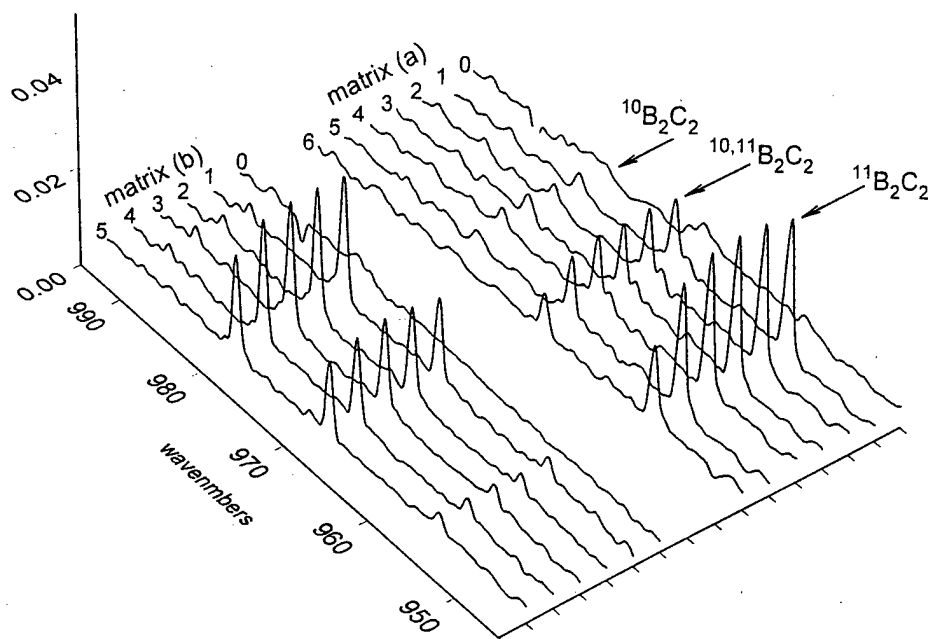
B2C2-3D May 28, 1999 8:31:14 AM

absorbance

$^{10}BC_2$

$^{11}BC_2$

0.06

0.04

0.02

0.00

1260

1242

1224

1206

1188

wavenmbers

matrix (a)

0 2 3 4 5 6

matrix (b)

0 1 2 3 4 5
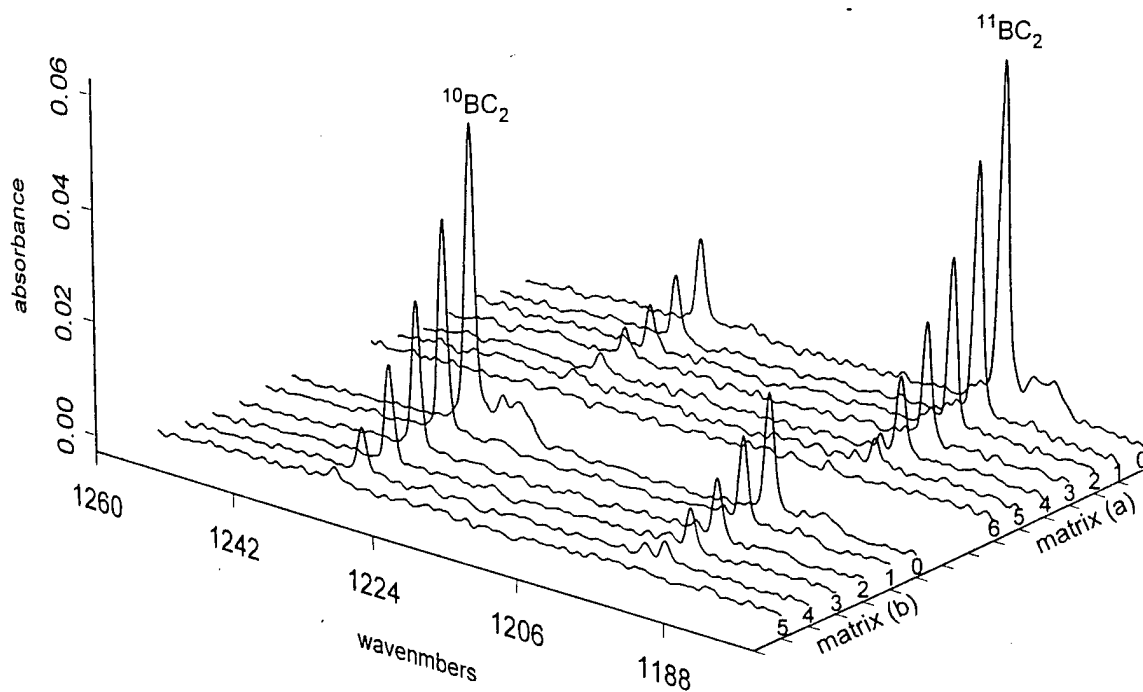
BC2rg3D  May 28, 1999  8:28:17 AM



0.02

0.01

0.00

matrix (a)

0 1 2 3 4 5 6

$C_4$

matrix (b)

0 1 2 3 4 5

$^{10}BC_3$

$^{11}BC_3$

1560

1550

1540

1530

1520

1510

1500

wavenmbers
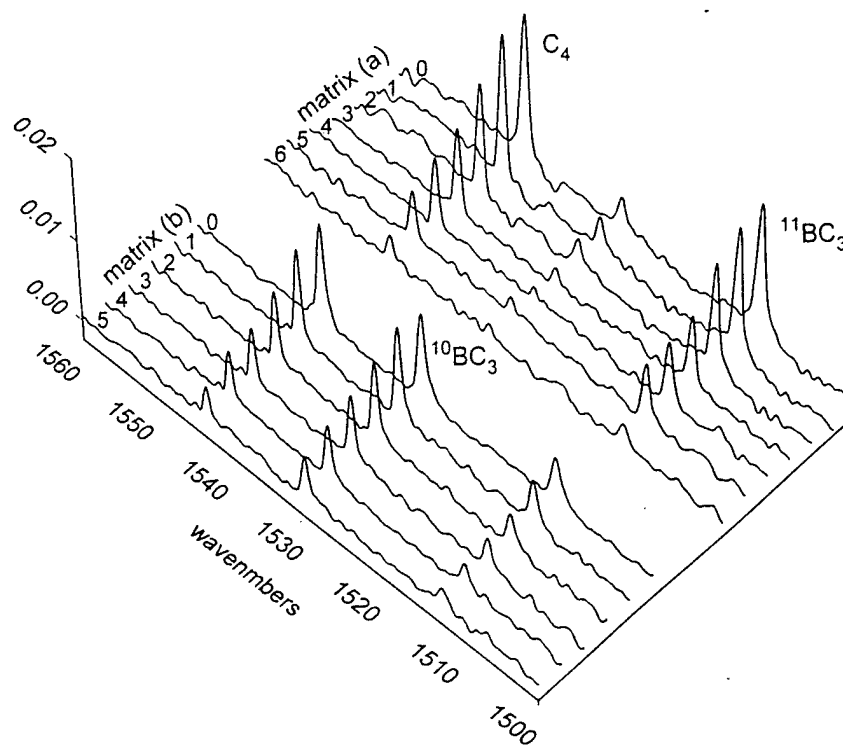
# Results and Discussion

Linear $C_3$, cyclic $BC_2$, and cyclic $B_2C$, constituted about 80% of the total observable boron and carbon in the initially deposited matrix, but $B_3$ was not observed.

The measured trimer distribution in the initially formed matrices was

$$\rho(C_3) : \rho(BC_2) : \rho(B_2C) : \rho(B_3) \sim 1 : 1.5 : 0.5 : < 0.05.$$

Statistical substitution of $J$ boron atoms into an $n$-atom carbon cluster produces a distribution given by $\rho(B_JC_{n-J})/ \rho(C_n) = [\{n(n-1)...(n-J+1)\}/J!] \, [B/C]^J$. With the experimental $B/C \sim 1/3$, the statistical trimer distribution is

$$\rho(C_3) : \rho(BC_2) : \rho(B_2C) : \rho(B_3) \sim 1 : 1 : 0.33 : 0.03.$$

Agreement between distributions implies trimers form by random condensation of well-mixed atoms, uninfluenced by the relative energies of the trimers, the energies of their precursors, or preferential kinetics pathways that could otherwise distort the statistics.

Linear $C_3$ and cyclic $BC_2$, disappeared entirely when the matrices were repeatedly annealed to temperatures between 25 K and 35 K, but cyclic $B_2C$ was inert.

Linear $C_4$ and $BC_3$ (BCCC) disappeared more slowly, and linear $B_2C_2$ (BCCB) grew to ~ 95% of its final value during the first annealing. $B_2C_2$ was also inert, as $B_2C$.

The sources of $B_2C_2$ are from condensation of atom plus trimer ($B + BC_2$ but not $C + B_2C$) or dimer + dimer ($BC + BC$ but not $B_2 + C_2$). Although BC was not observed, the upper limit of $\rho(BC)$ is larger than $\rho(B_2C_2)$ so that BC cannot be ruled out as a source of $B_2C_2$.

The growth of $B_2C_2$ is conclusive evidence of the presence of BC and/or B in the originally deposited matrix in an amount at least as great as the growth of $B_2C_2$.

Linear $C_5$, $BC_4$ ($BCCCC$) and $B_2C_3$ ($BCCCB$) and larger linear clusters ($B_JC_{n-J}$, $5 < n < 11$, $J = 0, 1, 2$), all grew upon annealing.

The sources of $B_2C_3$ are dimer + trimer ($BC + BC_2$ but not $B_2 + C_3$) and atom + tetramer ($B + BC_3$ but not $C + B_2C_2$).

Since $\rho(BC_2) \sim 5\rho(BC_3)$ in the initially deposited matrix, the $BC + BC_2$ source is dominant. Growth of $B_2C_3$ conclusively establishes the presence of BC in the matrix in an amount at least as great as the amount by which $B_2C_3$ grows.

Growth of $BC_4$ occurs primarily by $BC + C_3$ rather than $B + C_4$ or $C + BC_3$ because $\rho(C_3) \sim 10\rho(C_4)$ and $\rho(C_3) \sim 2\rho(BC_3)$. Growth of $C_5$ occurs by $C + C_4$ and $C_2 + C_3$, which establishes the presence of C and/or $C_2$ in the original matrix in an amount at least as great as $C_5$ growth.

Disappearance of triangular $BC_2$ requires breaking of one of its B-C bonds when one of its carbon atoms is attacked. The major reorganization of electronic energy involved in opening the ring appears to occur with little ($< \sim 3$ kcal mol$^{-1}$) or no energy barrier, which makes this small molecule a candidate for an interesting *ab-initio* study of unusual reactivity at low temperature.

# Goal

Production of Cryogenic HEDM with Five Mole Percent Atoms.

## Objective

Development and Characterization of Boron Atom Source.

## Approach

Production of HEDM by evaporation of boron with high-temperature graphite furnace and co-deposition of vapor with argon on a cold (10 K) surface

Identification and quantitative analysis of $B_J C_{n-J}$ species ($n \geq 3$, $J = 0$ to $n$) by FTIR spectroscopy and *ab-initio* calculations

Quantitative measurement of distributions of $B_J C_{n-J}$ species produced upon deposition and after annealing to a constant composition.

## Summary

Identities, structures and thermodynamic properties of $BC_2$, $B_2C$, $BC_3$, and $B_2C_2$ are conclusively established by isotope studies and matching experimental infrared spectra to predictions of theory.

Using the Standard Comparative Scheme adopted for the Isp of HEDM propellants (5 mole percent HEDM molecule in solid hydrogen) the predicted Isp of these new molecules stack up against the standards as follows:

## Summary (continued)

| | |
|---|---|
| Isp(LOX/LH2) | 389 sec |
| Isp(B atom) | 482 sec |
| Isp($B_2$) | 492 sec |
| Isp($BC_2$) | 482 sec |
| Isp($B_2C$) | 447 sec |
| Isp($BC_3$) | 439 sec |
| Isp($B_2C_2$) | 439 sec |

## Conclusions

Annealing kinetics of disappearance of $C_3$ and $BC_2$, and of appearance of $B_2C$, $C_4$, $BC_3$ $B_2C_2$, $C_5$, $BC_4$, and $B_2C_3$ unequivocally establishes the presence of atoms and dimers in the originally deposited matrix.

~ 80% or more of the initially deposited HEDM existed as atoms, dimers and trimers.

Molecules with two boron atoms are immune from radical attack and condensation during annealing.

## Future work

Continued development of source for production of higher flux beam of nearly pure boron atoms.

Map of "islands of stability" of pure boron HEDM; $B_2$ or $B_3$ may be the ultimate sink for atoms in the low temperature HEDM environment.

Determine reactivity of boron atoms with hydrogen during co-deposition.

Develop rapid condensation methodology to prevent reaction of B with $H_2$.